Interruption of Conjugation in Polyenes Bound to Transition-Metal Fragments

## John W. Chinn, Jr., and Michael B. Hall*

Contribution from the Department of Chemistry, Texas A&M University, College Station, Texas 77843. Received July 28, 1982

Abstract: In the past polyenes bound to transition-metal fragments were usually found to possess equal C–C bond lengths within experimental error. Recently, accurate studies of $(\eta^6\text{-}C_6H_6)Cr(CO)_3$, $(\eta^5\text{-}C_5H_5)Mn(CO)_3$, and $(\eta^5\text{-}C_5H_5)Co(CO)_2$ show that there is a pattern of short and long C–C bonds in these metal-bound polyenes. We have calculated the molecular orbitals of a large number of molecules in the series $(\eta^n\text{-}C_nH_n)M(CO)_m(XY)$ ($n = 3\text{–}7$, $m = 1\text{–}3$, $XY = CO$, N_2, NO, CN). Density difference plots show that the origin of these patterns in the C–C bond lengths is an intramolecular interruption of the conjugated π system of the polyene. The calculations suggest a general rule that C–C bonds in a polyene eclipsed below by a carbonyl or similar ligand will be long while those trans to these ligands will be short. These results are in agreement with recent accurate structures and even with some older structures where the significance of the differences in bond length is questionable. Exceptions to this rule occur for some room-temperature crystal structures in which the C–C distances are not precisely determined and for some systems in which there is a strong specific intermolecular interaction.

Introduction

There are numerous experimental and theoretical studies in the literature on organotransition-metal complexes having the general formula $(C_nR_n)ML_m$, where C_nR_n is a cyclic polyene which is bound in a π fashion to a transition-metal fragment, ML_m.[1] Of these polyenes, probably the most extensively studied class is that of benzene (Bz) and its derivatives, while the most extensively studied metal fragments are probably the metal tricarbonyls.[1a]

There is no question that benzene has a planar, regular, hexagonal structure in both the gaseous[2] and solid[3] states. Furthermore, this D_{6h} symmetry implies that benzene has a conjugated or delocalized π-bond system, and it has been argued whether this symmetry would be lowered when benzene was complexed to $Cr(CO)_3$, a species of C_{3v} symmetry.[4–9] The earliest solid-state structural studies of $(\eta^6\text{-benzene})$tricarbonylchromium(0), **1a**,

1a, M = Cr, R = H
b, M = Cr, R = CH₃
c, M = Mo, R = H
d, M = Cr, R = CH₃
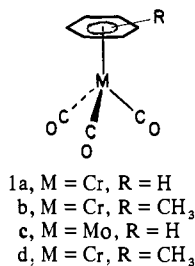
established that the complex existed in the staggered conformation **2** rather than the eclipsed conformation **3**,[4] and an early IR study suggested that the complexed benzene was reduced to threefold symmetry.[5] However, this was refuted by room-temperature

2   3
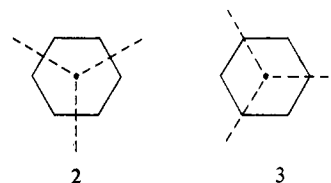
X-ray diffraction studies of **1a** and its hexamethyl derivative **1b** by Bailey and Dahl,[6] in which it was determined that the carbon–carbon (C–C) bond lengths were equal within three esd's (3σ) of the average value and that the arene was planar.[10] In addition, more recent IR and Raman experiments on **1a** and its derivatives indicated no distortion of the complexed arene.[7]

It was not until Rees and Coppens studied the solid state of **1a** at low temperature (78 K) with both X-ray and neutron diffraction that the structure was unambiguously solved.[8] Primarily, they found that the Bz fragment was distorted from a regular hexagon such that (1) the C–C bonds cis to (eclipsed by) the carbonyls were about 0.02 Å longer than those trans to the carbonyls and (2) the Bz fragment was not planar—i.e., the H atoms were displaced slightly (about 0.03 Å and 1.7°) out of the carbon plane toward the chromium. However, the distortions found in this solid-state study were considered to be insignificant in a subsequent gas-phase electron diffraction study of **1a**, in which the authors stated that the D_{6h} nature of the complexed benzene was "now so well established for chromium complexes in the vapor phase that any solution to the diffraction data involving a model with distorted C_6H_6 would be unacceptable".[9]

Because there still appears to be a controversy surrounding the geometry of **1a**, we decided to investigate its electronic structure theoretically, in hopes of providing a conclusive answer to the issue. Indeed, we wished to know if the features observed in the low-temperature diffraction study are true manifestations of the electronic structure of **1a** as an isolated molecule and not merely the effects of crystal packing forces. Furthermore, we desired to demonstrate that these deformations from regularity not only could be explained by a detailed analysis of the electronic in-

(1) See, for example: (a) Albright, T. A.; Hofmann, P.; Hoffmann, R. *J. Am. Chem. Soc.* **1977**, *99*, 7546. (b) Albright, T. A.; Hoffmann, R.; Tse, Y.; D'Ottavio, T. *Ibid.* **1979**, *101*, 3812. (c) Hoffmann, R. *Science (Washington, D.C.)* **1981**, *211*, 995.

(2) Electron diffraction: (a) Kimura, K.; Kubo, M. *J. Chem. Phys.* **1960**, *32*, 1776. (b) Bastiansen, O. *Acta Crystallogr.* **1957**, *10*, 861. Raman spectroscopy: (c) Langseth, A.; Stoicheff, B. P. *Can. J. Phys.* **1956**, *34*, 350. (d) Stoicheff, B. P. *Ibid.* **1954**, *32*, 339.

(3) Neutron diffraction: (a) Bacon, G. E.; Curry, N. A.; Wilson, S. A. *Proc. R. Soc. London, Ser. A* **1964**, *A279*, 98. X-ray diffraction: (b) Cox, E. G.; Cruickshank, D. W. J.; Smith, J. A. S. *Ibid.* **1958**, *A247*, 1.

(4) (a) Corradini, P.; Allegra, G. *J. Am. Chem. Soc.* **1959**, *81*, 2271. (b) Corradini, P.; Allegra, G. *Atti Accad. Naz. Lincei, Cl. Sci. Fis., Mat. Nat., Rend.* **1959**, *26*, 511. (c) Allegra, G. *Ibid.* **1961**, *31*, 241.

(5) Fritz, H. P.; Manchot, J. *Spectrochim. Acta* **1962**, *18*, 171.

(6) (a) Bailey, M. F.; Dahl, L. F. *Inorg. Chem.* **1965**, *4*, 1314. (b) *Ibid.* **1965**, *4*, 1298.

(7) (a) Cataliotti, R.; Poletti, A.; Santucci, A. *J. Mol. Struct.* **1970**, *5*, 215. (b) Brunvoll, J.; Cyvin, S. J.; Schäfer, L. *J. Organomet. Chem.* **1972**, *36*, 143. (c) Schäfer, L.; Begun, G. M.; Cyvin, S. J. *Spectrochim. Acta, Part A* **1972**, *28A*, 803.

(8) Rees, B.; Coppens, P. *Acta Crystallogr., Sect. B* **1973**, *B29*, 2516.

(9) Chiu, N.-S.; Schäfer, L.; Seip, R. *J. Organomet. Chem.* **1975**, *101*, 331.

(10) It should be noted here that all comments regarding the presence or absence of distortions in a structural study are made with reference to the 3σ test of statistical significance. Thus, experimental values within three estimated standard deviations (esd's) of one another are the same (equal), and those outside of 3σ are different (unequal) within a 99.7% level of confidence.

teractions involved but also could be illustrated clearly and simply with deformation density ($\Delta\rho$) maps. The method we will use in our deformation density study is unique, in that we will subtract the theoretical densities of component molecular fragments from the total density of the complex, all of which are in idealized, regular geometries.[11-13] In this way we should be able to observe more easily how each fragment perturbs the electronic structure of the other in the formation of the stable complex.

This approach is in contrast to the method most often employed in $\Delta\rho(\mathbf{r})$ studies.[14] Experimentalists subtract the superposition of the best theoretical, spherical, ground-state atoms[15] from the experimental electron density distribution, $\rho(\mathbf{r})$ (as determined by X-ray diffraction), at the positions found either from neutron or high-order X-ray diffraction data.[13,14a-e] Theoreticians usually subtract the superposition of the best spherical, ground-state atoms from the theoretical electron density distribution, $\langle\psi|\rho(\mathbf{r})|\psi\rangle$.[11,12,14] Interpretation of both the experimental and theoretical results is hampered by the fact that subtraction of the atoms causes the resultant $\Delta\rho(\mathbf{r})$ maps to display the gross deformations of the atomic electron distributions, while the finer and often more interesting details which may be associated with fragment interaction or geometric configuration are obliterated.[14]

By subtracting the theoretical densities of the molecular fragments from the total density of the complex, we have minimized the effects of most of the foregoing problems. Since the wave functions of the complex and its component fragments are generated within the same limitations of the basis set and calculational technique chosen, most errors involved are largely cancelled on computing $\Delta\rho(\mathbf{r})$. Furthermore, each fragment has already incorporated many of the gross electron density shifts associated with bond formation into its electron density, and so our $\Delta\rho(\mathbf{r})$ maps tend to reflect the subtler density changes which occur both at the interface of the fragments during complexation, as well as within those fragments after complexation.
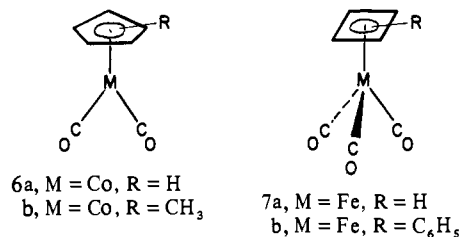
The theoretical basis for our method lies in the electrostatic theory of Hellmann and Feynman,[16] which was further developed by Nakatsuji into his electrostatic force theory.[17,18a,b] In his studies of simple polyatomic systems, he found that when the atoms in a molecule were displaced from their equilibrium geometry, the resulting $\rho(\mathbf{r})$ relocalized toward those regions of space vacated

by the atoms in question. This, then, provided a restoring force acting on the displaced atoms to return them to their original positions. This concept—that the centroid of the electron density near a nucleus will precede the movement of that nucleus—was termed "electron-cloud preceding".[17,18c-g]

In this study, we will apply the concept of *electron density leading*[17] to a study of cyclic polyenes (C_nH_n, n = 3-7) bound to transition-metal fragments of the type ML_m (m = 2-4). We will show that counterligands (L) such as CO will interrupt the π-bond conjugation in the cyclopolyene, causing the C-C bonds cis to L to be longer than those trans to L, and why this occurs. A detailed analysis of the electronic structure of **1a** will be presented first to establish the validity and success of the method. These results will be compared to calculations of the isolobal (η^6-C$_6$H$_6$)Mo(CO)$_3$, **1c**, to examine the effects of the larger metal on the size and direction of the deformations. Next, the isoelectronic series (η^6-C$_6$H$_6$)Cr(CO)$_2$XY [XY = N$_2$, CN$^-$, NO$^+$], **4**, will be studied to compare how each of the four counterligands (CO, N$_2$, CN$^-$, NO$^+$) affects the bonding in the complexed benzene.

4a, L = N$_2$
b, L = CN$^-$
c, L = NO$^+$

5a, M = Mn
b, M = Re
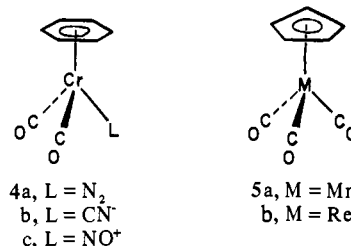
The technique will then be applied to a study of (η^5-cyclopentadienyl)tricarbonylmanganese(I), **5a**, (η^5-cyclopentadienyl)dicarbonylcobalt(I), **6a**, and (η^4-cyclobutadiene)-tricarbonyliron(0), **7a**. Early ambient-temperature X-ray

6a, M = Co, R = H
b, M = Co, R = CH$_3$

7a, M = Fe, R = H
b, M = Fe, R = C$_6$H$_5$

structures of **5a**[19] and **7b**[20a] (the tetraphenyl derivative of **7a**) displayed distortions in the polyene C-C bond-lengths which were not in keeping with the ideal local symmetry of the free complex. However, they were considered not to be significant because the C-C bond lengths were equal within experimental error. Even more recent studies on **5a** (including one at 115 K)[21] and its rhenium analogue **5b**[22] have not reduced the distortions from the highest ideal symmetry in this species. Since it is not clear whether these distortions are due to intermolecular packing forces or intramolecular electronic factors, the present deformation density studies should help to explain the causes of some of them and to indicate which ones are true deformations of the electronic structure of the free complex. Also, though an X-ray structure of **6a** has never been performed, recent gas-phase electron diffraction work on **6a** and an X-ray crystal study of **6b**[23b] have revealed definite distortions in the C-C bonds of the complexed

(11) Some theoretical studies have been performed on rotational barriers in simple organic molecules, in which the electron densities of conformers have been subtracted to observe the density shifts in the bond about which rotation occurred. See, for example: (a) Payne, P. W. *J. Chem. Phys.* **1978**, *68*, 1242. (b) Absar, I.; Van Wazer, J. R. *Ibid.* **1972**, *56*, 1284. (c) Jorgensen, W. L.; Allen, L. C. *J. Am. Chem. Soc.* **1971**, *93*, 567.

(12) A similar theoretical approach has been employed to study (1) hydrogen binding between simple molecules (by subtracting $\langle\rho(\mathbf{r})\rangle$ of the individual molecules from that of the associated "supermolecule"): (a) Kerns, R. C.; Allen, L. C. *J. Am. Chem. Soc.* **1978**, *100*, 6587. (b) Kollman, P. A.; Allen, L. C. *Ibid.* **1970**, *92*, 6101. (2) The effects of fluorine substitution in cyclopropane: (c) Deakyne, C. A.; Allen, L. C.; Craig, N. C. *Ibid.* **1977**, *99*, 3895.

(13) A few research groups have attempted to calculate molecular form factors to achieve a better fit of the experimental density: (a) Groenewegan, P. P. M.; Feil, D. *Acta Crystallogr., Sect. A* **1969**, *A25*, 444. (b) Jones, D. S.; Lipscomb, W. N. *Ibid.* **1970**, *A26*, 196.

(14) For a broad review of the experimental and theoretical aspects of obtaining charge and deformation densities, see: (a) Coppens, P. *Int. Rev. Sci.: Phys. Chem., Ser. 2* **1975**, *11*, 21. (b) Coppens, P.; Stevens, E. D. *Adv. Quantum Chem.* **1977**, *10*, 1. (c) Becker, P. *Phys. Scr.* **1977**, *15*, 119. (d) Hirshfeld, F. L., Ed. *Isr. J. Chem.* **1977**, *16*, 87. (e) Coppens, P. *Top. Curr. Phys.* **1978**, *6* (Neutron Diffraction), 71. (f) Smith, V. H., Jr. *Phys. Scr.* **1977**, *15*, 147. (g) Rees, B. *Acta Crystallogr., Sect. A* **1978**, *A34*, 254. (h) Hansen, N. K.; Coppens, P. *Ibid.* **1978**, *A34*, 909. (i) Coppens, P., Hall, M. B., Eds. "Electron Distributions and the Chemical Bond"; Plenum Press: New York, 1982.

(15) More precisely, these are theoretical atomic X-ray form (scattering) factors. This superposition is often referred to as the "promolecule"—Hirschfeld, F. L.; Rzotkiewicz, S. *Mol. Phys.* **1974**, *27*, 1319.

(16) (a) Hellmann, H. "Einführung in die Quantenchemie"; Deuticke: Vienna, 1937. (b) Feynman, R. P. *Phys. Rev.* **1939**, *56*, 340.

(17) Nakatsuji, H. *J. Am. Chem. Soc.* **1973**, *95*, 2084.

(18) (a) Nakatsuji, H. *J. Am. Chem. Soc.* **1973**, *95*, 345. (b) *Ibid.* **1973**, *95*, 354. (c) Nakatsuji, H.; Kuwata, T.; Yoshida, A. *Ibid.* **1973**, *95*, 6894. (d) Nakatsuji, H. *Ibid.* **1974**, *96*, 24. (e) *Ibid.* **1974**, *96*, 30. (f) Koga, T.; Nakatsuji, H.; Yonezawa, T. *Ibid.* **1978**, *100*, 7522. (g) Nakatsuji, H.; Kanayama, S.; Harada, S.; Yonezawa, T. *Ibid.* **1978**, *100*, 7528.

(19) Berndt, A. F.; Marsh, R. E. *Acta Crystallogr.* **1963**, *16*, 118.

(20) (a) Dodge, R. P.; Schomaker, V. *Acta Crystallogr.* **1965**, *18*, 614. (b) Davis, M. I.; Speed, C. S. *J. Organomet. Chem.* **1970**, *21*, 401.

(21) (a) Fitzpatrick, P. J.; Le Page, Y.; Sedman, J.; Butler, I. S. *Inorg. Chem.* **1981**, *20*, 2852. (b) Fitzpatrick, P. J.; Butler, I. S., McGill University, personal communication.

(22) Fitzpatrick, P. J.; Le Page, Y.; Butler, I. S. *Acta Crystallogr., Sect. B* **1981**, *B37*, 1052.

(23) (a) Beagley, B.; Parrott, C. R.; Albrecht, V.; Young, G. G. *J. Mol. Struct.* **1979**, *52*, 47. (b) Byers, L. R.; Dahl, L. F. *Inorg. Chem.* **1980**, *19*, 277.

4932   *J. Am. Chem. Soc., Vol. 105, No. 15, 1983*

Chinn and Hall

Table I. Molecular Geometries Used in the Isoelectronic Series Calculations[a]

parameter	(C_nH_n)-$M(XO)_2$[b]	(C_nH_n)-$M(XO)_3$[c]
r_{M-CH}	2.10	2.20
r_{M-XO}	1.70	1.80
r_{X-O}	1.14	1.15
r_{C-C}	1.41	1.41
r_{C-H}	1.10	1.10
$\angle M-X-O$	180	180
$\angle X-M-X$	109.5[d]	90

[a] Bond lengths are in Å and bond angles in degrees. [b] X = C, N. [c] X = C. [d] Actual tetrahedral angle value of $\cos^{-1} (-1/3)$ used.

cyclopentadienyl ligand, and we will discuss those findings in light of this work.

Finally, the method will be used to examine the series of isoelectronic, first-row transition-metal complexes $(C_nH_n)M(CO)_m$ [n = 3–7; m = 2–4], so that we can comment on the applicability of this technique to predicting structural (and maybe reactivity) patterns of these complexes, some of which are not yet known.

Theoretical Considerations

Method. Nonempirical, Hartree–Fock MO calculations were performed on these complexes by using the self-consistent field (SCF) Fenske–Hall approach, program MEDIEVAL, which has been discussed in detail elsewhere.[24] Though approximate in nature, the method is parameter free, and the final results depend only upon the chosen atomic basis set and internuclear distances. Because the technique is principally used to analyze qualitative trends over a series of related molecules (for which it is well suited),[25] it is not necessary to use the exact bond lengths and angles for the compounds being studied. As long as major differences in metal size, metal charge, or counterligand (L) type are accounted for, bond length variations of ±0.05 Å and bond angle variations of ±5° will produce the same trends.

SCF calculations were performed in the atomic basis on the C_nH_n, L, and ML_m fragments and on the $(C_nH_n)ML_m$ complexes. To aid in the interpretation of the atomic orbital (AO) interactions, the converged wave function was transformed to appropriate fragment MO bases. These wave functions were then used in program MOPLOT[26] to generate total electron density ($\langle \psi | \rho(\mathbf{r}) | \psi \rangle$) maps of both the complexes and their component fragments in various regions of space. The fragment maps were summed together, and that sum was subtracted from the total density of the complex to yield the deformation density.

$$\Delta\rho(\mathbf{r}) = \rho(\mathbf{r})_{complex} - \sum_i \rho(\mathbf{r})_{fragment_i} \qquad (1)$$

The $\Delta\rho$ maps were plotted by using program CONTOUR.[27] In the plots, solid lines represent positive density contours and dashed lines represent negative contours. The calculations were carried out on the university's Amdahl 470V/6 and V/7 computers, and the plotting was done on a Versatec Model 1200 plotter.

Geometry. On the basis of a survey of the best structural data available,[30] idealized regular geometries were chosen for the
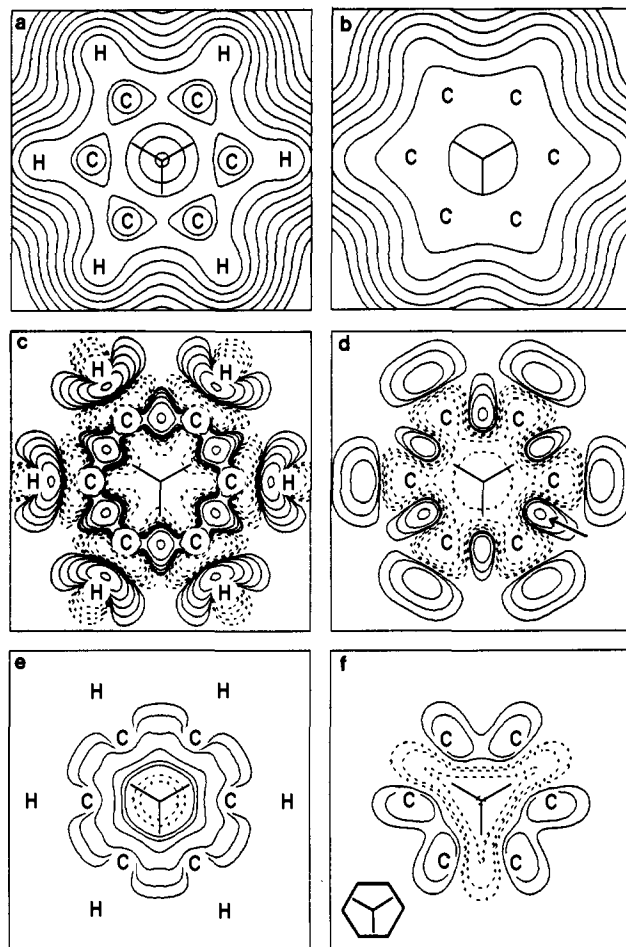
Figure 1. Electron density plots for $(Bz)Cr(CO)_3$ in the staggered conformation: (a) is the total density in the plane of the benzene ring, (b) is the total density in a plane between Cr and Bz near the π-maximum for the carbon 2p orbitals, (c) is the atomic deformation density in the plane of (a), (d) is the atomic deformation density in the plane of (b), (e) is the fragment deformation density in the plane of (a), and (f) is the fragment deformation density in the plane of (b).

complexes and fragments under study, such that three criteria were satisfied: (1) the cyclopolyene (C_nH_n) was treated as a planar, regular n-gon, (2) the ML_m fragment was given C_{mv} symmetry, and (3) the polyene was kept periplanar to the L_m plane. The geometries used in the calculations are summarized in Table I. Calculations were performed on these complexes in both the staggered and eclipsed conformations.[31]

Basis. Slater-type functions for the first-row elements were taken from Clementi's double-ζ functions for neutral atoms,[32] in which all but the outer 2p orbitals were curve fit to orthonormal single-ζ functions using the maximum overlap criterion.[33] The 2p functions were kept double-ζ. A 1s exponent of 1.2 was used for hydrogen.[34] The first- and second-row transition-metal

(24) Hall, M. B.; Fenske, R. F. *Inorg. Chem.* **1972**, *11*, 768.

(25) See, for example: (a) Hall, M. B.; Fenske, R. F. *Inorg. Chem.* **1972**, *11*, 1619. (b) Sarapu, A. C.; Fenske, R. F. *Ibid.* **1975**, *14*, 247. (c) Yarbrough, L. W., II; Hall, M. B. *Ibid.* **1978**, *17*, 2269. (d) Sherwood, D. E., Jr.; Hall, M. B. *Ibid.* **1980**, *19*, 1805.

(26) Lichtenberger, D. L. Ph.D. Dissertation, University of Wisconsin, Madison, Wisconsin, 1974. Program available from QCPE (No. 284), Chemistry Department, Indiana University, Bloomington, IN 47401.

(27) An in-house program which uses CONREC, a special smoothing routine for drawing contours, developed at the National Center for Atmospheric Research (NCAR), Boulder, Colorado, and adapted for use on the Amdahl 470V/6 by Thomas Reid, Data Processing Center, Texas A&M University.

(28) Koshland, D. E.; Myers, S. E.; Chesick, J. P. *Acta Crystallogr., Sect. B* **1977**, *B33*, 2013.

(29) (a) Riley, P. E.; Davis, R. E. *J. Organomet. Chem.* **1976**, *113*, 157. (b) Rausch, M. D.; Westover, G. F.; Mintz, E.; Reisner, G. M.; Bernal, I.; Clearfield, A.; Troup, J. M. *Inorg. Chem.* **1979**, *18*, 2605.

(30) (a) See ref 1a, 6, 8–9, 19–23, 28–29, 38, 43, 48, 50, 52, 54, 59, 61–63. (b) Brauer, D. J.; Krüger, C. *J. Organomet. Chem.* **1972**, *42*, 129. (c) Avdeef, A.; Raymond, K. N.; Hodgson, K. O.; Zalkin, A. *Inorg. Chem.* **1972**, *11*, 1083. (d) Gard, E.; Haaland, A.; Novak, D. P.; Seip, R. *J. Organomet. Chem.* **1975**, *88*, 181. (e) van Meurs, F.; Van Koningsveld, H. *Ibid.* **1975**, *118*, 295. (f) Cowman, C. D.; Thibeault, J. C.; Ziolo, R. F.; Gray, H. B. *J. Am. Chem. Soc.* **1976**, *98*, 3209. (g) Cann, K.; Riley, P. E.; Davis, R. E.; Pettit, R. *Inorg. Chem.* **1978**, *17*, 1421. (h) Hossain, M. B.; van der Helm, D. *Ibid.* **1978**, *17*, 2893. (i) Adams, M. A.; Folting, K.; Huffman, J. C.; Caulton, K. G. *Ibid.* **1979**, *18*, 3020.

(31) In the staggered conformation, the counterligands eclipse mostly C–C bonds. In the eclipsed conformation, the counterligands eclipse mostly carbon atoms.

(32) (a) Clementi, E. *J. Chem. Phys.* **1964**, *40*. (b) Clementi, E. *IBM J. Res. Dev.* **1965**, *9*, 2; and its supplement: "Tables of Atomic Functions".

(33) (a) Radtke, D. D. Ph.D. Dissertation, University of Wisconsin, Madison, WI, 1966. (b) Fenske, R.; Radtke, D. *Inorg. Chem.* **1968**, *7*, 479.

Polyenes Bound to Transition-Metal Fragments

J. Am. Chem. Soc., Vol. 105, No. 15, 1983 4933

functions used were those of Richardson et al.[35] and were augmented by 4s and 4p exponents of 2.0 for the first-row metals and by 5s and 5p exponents of 2.2 for the second-row metals.[36]

Results and Discussion

η^6-Benzene (Bz) Complexes. In the low temperature study of **1a** by Rees and Coppens, the complex was shown to exhibit the staggered conformation **2** with the C–C bonds eclipsed by the carbonyls averaging 1.423 (2) Å and those trans to the carbonyls averaging 1.407 (2) Å.[8] Thus, the eclipsed carbon bonds are longer than those trans to the carbonyls. This bond length difference should be reflected in the electron density of the complex. Figure 1 shows density plots, $\rho(\mathbf{r})$, for **1a** both in the benzene σ plane and near the radial π maximum for carbon 2p orbitals between the Cr and Bz. The total density plots (Figure 1a,b) both emphasize the hexagonal shape of the complexed Bz but give no hint to the presence of any bond alternation.

Parts c and d of Figure 1 represent density difference plots ($\Delta\rho$) of the same planes in which spherical ground-state atoms were subtracted from the total density. In the particular plots illustrated, the Cr was in a $(4s^0 3d^6)$ configuration. No detectable difference was found for Cr in a $(4s^1 3d^5)$ configuration. As with the total density maps, there is no indication of the C_{3v} nature of the complex evident in the σ-plane map, though there are peaks of positive density in the C–C and C–H bonding regions. The π-maximum plane, however, seems to suggest that there may be more electron density in the trans C–C bonds, as indicated by the presence of an extra contour in those bonding regions.

The $\Delta\rho$ plots generated by subtracting the fragment electron densities of Bz and Cr(CO)$_3$ from the total are shown in Figure 1e,f, again for the same two planes. Apart from the observation that the C–C σ-bond framework gains electron density from the Cr(CO)$_3$ fragment, the map of the Bz plane has no other distinctive features, indicating the bond alternation is not controlled by the molecular orbitals involved in C–C and C–H σ bonding. On the other hand, the π-maximum plane dramatically reveals the density gain in the trans C–C bonds of the complexed Bz, relative to free benzene. This is clear evidence that the eclipsed C–C bonds will be longer than those trans to the carbonyls (as seen in the structure) and points out that the bond alternation in **1a** is due to internal electronic forces and not to solid-state forces. Further evidence of the bond alternation is displayed by the differences in the π-overlap populations of the cis and trans C–C bonds, as shown in Table II, and agrees with the calculations of Rees and Coppens.[8]

A clue to the cause of this bond alternation is revealed upon examination of plots perpendicular to the Bz and through the midpoints of the C–C bonds. The slices in Figure 2a,b contain one of the carbonyl groups and bisect the other two. Again, the map produced by subtracting spherical atoms indicates both π regions should be nearly the same, whereas the one generated by subtracting fragments produces a region of large density loss below the eclipsed C–C bond and a region of density gain below the trans C–C bond. Thus, it appears that the eclipsing carbonyl is interacting strongly with the benzene π-bond system, in either a through-bond or through-space fashion. Upon closer examination of the interactions, we find that the carbonyl 2π-acceptor orbitals couple strongly with the metal $d_{x^2-y^2}$ and d_{xy} (and to some extent the d_{xz} and d_{yz} orbitals), which thereby interact with the Bz HOMO ($1e_{1g}$) and LUMO ($1e_{2u}$) orbitals to direct electron density out of the cis C–C bonds and into the trans bonds. This will be discussed more completely later.

Having verified the electronic nature of the bond alternation, we were interested in seeing if the slight displacement of the C–H
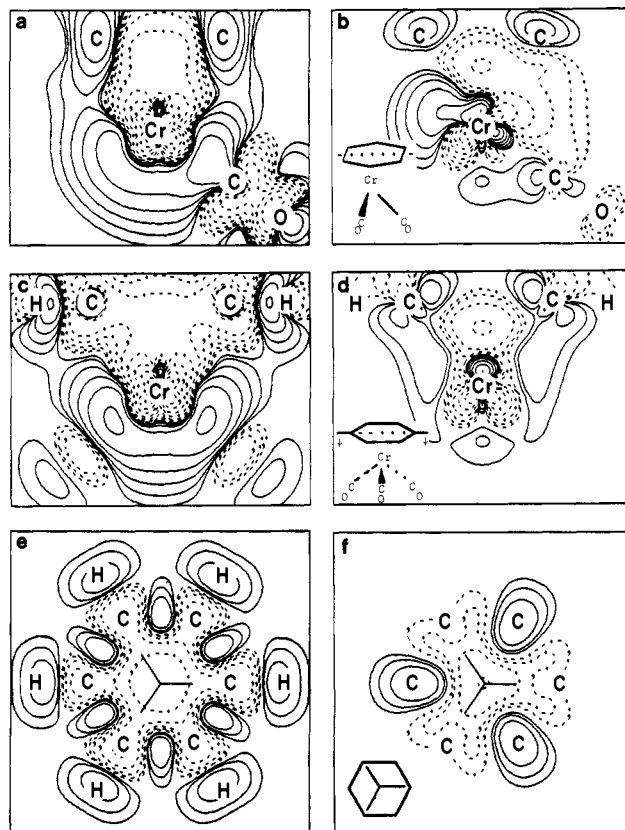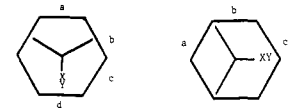
(34) Hehre, W. J.; Stewart, R. F.; Pople, J. A. *J. Chem. Phys.* **1969**, *51*, 2657. The value used represents the best average for hydrogen for all but the most polar bonding situations.

(35) (a) Richardson, J.; Nieuwpoort, W. C.; Powell, R. R.; Edgell, W. F. *J. Chem. Phys.* **1962**, *36*, 1057. (b) Richardson, J.; Blackman, M.; Ranochak, J. *Ibid.* **1973**, *58*, 3010.

(36) These values were chosen because they give maximum σ overlap with the ligand functions, and past experience has shown that they give reasonable results.

Figure 2. Deformation density plots of (Bz)Cr(CO)$_3$. The plane for maps a and b is perpendicular to the Bz ring and passes through the Cr atom and one of the carbonyls. This plane passes through the midpoints of two opposite C–C bonds in the Bz ring: (a) is the atomic deformation density and (b) is the fragment deformation density. The plane for maps c and d is perpendicular to the Bz ring and contains the Cr atom and two opposite C–H bonds in the Bz ring. Map c is the atomic deformation density while map d is the fragment deformation density. Maps e and f are similar to those in Figure 1e,f except that the (Bz)Cr(CO)$_3$ is now in the eclipsed conformation.

bonds out of the plane could be predicted from the fragment deformation densities. Hoffmann has stated that displacement of the substituents depends upon the size of the ring.[1a,37a] Six-membered rings and larger must rotate their carbon p orbitals inward for good overlap with the metal d orbitals, whereas for five-membered rings and smaller, the p orbitals must be rotated outward for good overlap. Thus, the H's on complexed Bz should move downward and the H's on complexed cyclobutadiene should move upwards. If we examine plots through the C–H bond and perpendicular to the Bz plane (Figure 2c,d), we see that this is indeed what happens. In the fragment $\Delta\rho$ map (Figure 2d) there is density loss above the C–H bond, and so the hydrogen will want to move downward toward the Cr into the region of the positive density; i.e., the residual electron density leads the H's away from planarity. In fact, one can even see the rotation of the carbon 2p orbitals in this plot. Compare that to the atom $\Delta\rho$ plot (Figure 2c) which does not show a preference for the hydrogen moving at all. The fragment map clearly indicates that the displacement of the H's toward the Cr is due to internal electronic forces and not to solid-state effects.

Hoffmann and others have also shown that the rotational barrier in **1a** is very small,[4] and it is not surprising that a number of substituted (Bz)M(CO)$_3$ complexes have the eclipsed conformation **3** in the solid state. In light of this, calculations were also done on the eclipsed conformer of **1a**. The $\Delta\rho$ maps (Figure 2d,f) and π-overlap populations (Table II) of the complex revealed no bond alternation, which is to be expected since the C–C bonds are now

(37) (a) Elian, M.; Chen, M. M. L.; Mingos, D. M. P.; Hoffmann, R. *Inorg. Chem.* **1976**, *15*, 1148. (b) Elian, M.; Hoffmann, R. *Ibid.* **1975**, *14*, 1058.

4934 *J. Am. Chem. Soc., Vol. 105, No. 15, 1983*

Chinn and Hall

Table II. Calculated π-Overlap Populations of the C–C Bonds of (Bz)M(CO)₂(XY) Complexes in the Staggered and Eclipsed Conformations

		conformation						
		staggered				eclipsed		
M	XY	a	b	c	d	a	b	c
Cr	CO	0.130	0.110	0.130	0.110	0.120	0.120	0.120
	N₂	0.128	0.109	0.130	0.109	0.120	0.118	0.121
	CN⁻	0.126	0.110	0.132	0.105	0.121	0.114	0.121
	NO⁺	0.129	0.108	0.126	0.113	0.117	0.120	0.119
Mo	CO	0.131	0.109	0.131	0.109	0.120	0.120	0.120

equivalent electronically. The primary difference between conformers **2** and **3** is the charge on the carbon atoms (Table III). Both the fragment $\Delta\rho$ maps and the atomic charges indicate that there is a significant loss of electron density at the eclipsed carbons, resulting in an increase in the p_π density for the trans carbons.

The importance of this observation, which Hoffmann also recognized,[1a] is twofold. First, we would expect that, structurally, the carbonyls would tend to rotate toward and eclipse carbons substituted with electron-donating groups (provided the groups are not too large) and away from carbons substituted with electron-withdrawing groups; i.e., M(CO)₃ groups would rotate toward electron density enhanced and away from electron density depleted carbons. This is found in (η^6-1,3,5-trimethylbenzene)tricarbonylmolybdenum(0), **8**,[28] and (η^6-toluene)tricarbonylchromium(0), **9**,[38b] where the carbonyls eclipse the methyl groups, and in (η^6-methyl benzoate)Cr(CO)₂L [L = CO, CS], **10** and **11**,[38a,c] where the ester group bisects the carbonyls. Second, we

10, L = CO
11, L = CS
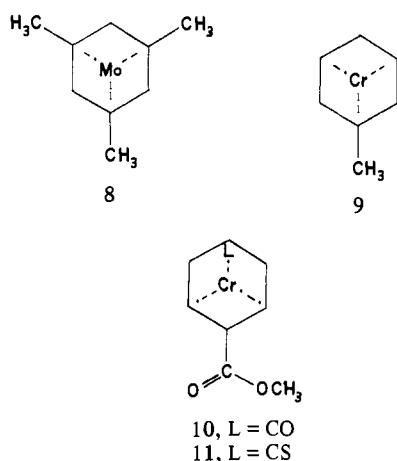
would expect this aspect to play an important part in the solution chemistry of substituted (Bz)M(CO)₃ complexes. Because of its low rotational barrier, the M(CO)₃ group would rotate to an eclipsed conformation, so that nucleophiles could attack the eclipsed carbons and electrophiles could attack the uneclipsed carbons. Indeed, one might tie down one end of the complex with a bulky group to force it into a preferred orientation for selective reactivity at certain carbons.

This phenomenon has been investigated considerably, both experimentally[39,40] and theoretically.[41] Semmelhack and co-

(38) (a) Saillard, J.-Y.; Le Borgne, G.; Grandjean, D. *J. Organomet. Chem.* **1975**, *94*, 409. (b) van Meurs, F.; van Koningsveld, H. *Ibid.* **1977**, *131*, 423. (c) Saillard, J.-Y.; Grandjean, D. *Acta Crystallogr., Sect. B* **1976**, *B32*, 2285.
(39) (a) Semmelhack, M. F.; Bisaha, J.; Czarny, M. *J. Am. Chem. Soc.* **1979**, *101*, 768. (b) Semmelhack, M. F.; Clark, G. R.; Farina, R.; Saeman, M. *Ibid.* **1979**, *101*, 217. (c) Semmelhack, M. F.; Clark, G. *Ibid.* **1977**, *99*, 1675. (d) Semmelhack, M. F.; Thebtaranonth, Y.; Keller, L. *Ibid.* **1977**, *99*, 959. (e) Semmelhack, M. F.; Hall, H. T., Jr.; Yoshifuji, M. *Ibid.* **1976**, *98*, 6387.

Scheme I

R = Me, Et, OMe, NMe₂

Scheme II

R = CMe₃, SiMe₃, CH(t-Bu)₂, CF₃

workers found that nucleophilic substitution on (arene)tricarbonylchromium complexes shifted from primarily meta attack (Scheme I, path 1) to primarily para attack (Scheme II, path 1) as the electron-donating group (R) became increasingly bulkier.[39] Similarly, Jackson and Jennings found that electrophilic attack occurred more at the meta position (Scheme II, path 2) and less at the ortho and para positions (Scheme I, path 2) as the steric bulk of the R group increased.[40] Thus, for small R substituents on the complexed arene, the Cr(CO)₃ group will rotate to eclipse the R-substituted carbon (Scheme I), causing the eclipsed meta positions to be electron density depleted and the staggered ortho and para positions to be, likewise, electron density enhanced. Therefore, nucleophiles attack the meta carbons, and electrophiles attack the ortho and para carbons. As R becomes bulkier, steric repulsion forces the Cr(CO)₃ group into a conformation where the ortho and para positions are now eclipsed by carbonyls (Scheme II). However, the same density arguments apply: nucleophiles attack the density depleted (eclipsed) ortho and para carbons, and electrophiles attack the density enhanced (staggered or trans) meta carbons. Scheme II would also be followed for electron-withdrawing R groups, yielding the same results. Thus, we can generally say that in (arene)M(CO)₃ complexes, bonds (atoms) which are eclipsed by (or cis to) carbonyls are electron density depleted and bonds (atoms) which are trans to carbonyls are electron density enhanced, relative to the free arene.

With the advent of the structural work by Koshland et al.,[28] on **8** and (η^6-hexamethylbenzene)tricarbonylmolybdenum(0), **1d**, which indicated (1) equal C–C bonds in the eclipsed structure of **8**, (2) alternating C–C bond lengths in the staggered structure of **1d** (with a difference of 0.036 Å), and (3) displacement of the methyl groups away from the Mo (0.035 Å in **8** and 0.060 Å in **1d**) calculations were also done on the staggered and eclipsed conformers of the parent species **1c**. Not surprising, the results are very similar to those for **1a**, but the π-maximum plane does

(40) Jackson, W. R.; Jennings, W. B. *Chem. Commun.* **1966**, 824.
(41) (a) Albright, T. A.; Carpenter, B. K. *Inorg. Chem.* **1980**, *19*, 3092 and references therein. (b) Solladie-Caballo, A.; Wipff, G. *Tetrahedron Lett.* **1980**, *21*, 3047.

Table III. Calculated Atomic Charges on the Bz Carbon Atoms in $(Bz)M(CO)_2(XY)$ Complexes in the Staggered and Eclipsed Conformations

		conformation						
		staggered			eclipsed			
M	XY	a	b	c	a	b	c	d
Cr	CO	−0.033	−0.033	−0.033	−0.079	0.012	−0.079	0.012
	N_2	−0.033	−0.029	−0.038	−0.079	0.017	−0.085	0.013
	CN⁻	−0.067	−0.056	−0.059	−0.106	−0.015	−0.116	0.003
	NO⁺	0.000	−0.001	−0.003	−0.047	0.043	−0.038	0.030
Mo	CO	−0.032	−0.032	−0.032	−0.079	−0.015	−0.079	0.015

show a tendency for **1c** to have a larger C–C bond length difference, as was observed in the permethyl complex **1d**.[28]

Finally, we were interested in studying this interruptive effect which the carbonyl has upon the complexed Bz to see if other isoelectronic ligands behave the same way. In particular, we examined $(Bz)Cr(CO)_2(XY)$, $[XY = N_2, CN^-, NO^+]$, **4**, in both the staggered and eclipsed conformers. From these results we can generalize (1) that all four ligands (CO, N_2, CN⁻, and NO⁺) can act to interrupt the conjugation of the complexed polyene in the same way, (2) that there is little difference between CO and N_2 (no surprise), (3) that CN⁻ withdraws much less density than CO from the π region, and (4) that NO⁺ withdraws much more density than CO from the π region. Furthermore, there is a good possibility that one could detect four distinct C–C bond lengths in the staggered conformer of either a $(Bz)M(CO)_2(CN)$ or a $(Bz)M(CO)_2(NO)$ complex, such as $(Bz)Mn(CO)_2(CN)$ or $(Bz)V(CO)_2(NO)$. Finally, we would expect that the eclipsed conformation of the CN complex to exhibit preferential reactivity with electrophiles and the NO complex to exhibit preferential reactivity with nucleophiles, compared to the CO complex.

It is worth mentioning that at least one study has indicated that dinitrogen (N_2) is a weaker π acceptor, but stronger $(\sigma + \pi)$-electron donor, than carbonyl in the $(Bz)Cr(CO)_2(XY)$ $[XY = N_2, CO]$ complexes.[42] This is subtly observed in our results, where CO does withdraw more electron density than N_2 from the polyene framework. (Conversely, one could say that N_2 feeds more electron density than CO into the polyene.)

Based upon what we have just observed for the $(Bz)ML_3$ systems, what would one expect to find for benzene complexed to ML_2 or ML_4 fragments? For $(Bz)ML_2$ complexes, such as $(Bz)Cr(NO)_2$, $(Bz)Mn(CO)(NO)$, or $(Bz)Fe(CO)_2$, the two principle structural conformers are **12** and **13**. Using the idea

12

13
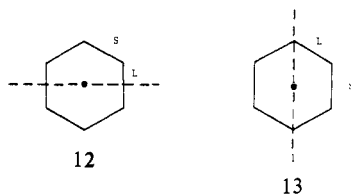
that the eclipsed C–C bonds are longer, we would expect to find two equal long bonds and four equal shorter bonds in **12**, producing an electronic structure like **14**, a six-membered ring with two allylic-like ends. Similarly, four equal long bonds and two equal shorter bonds would be expected in **13**, generating a structure such as **15**, a six-membered ring with two olefinic-like sides.

14   **15**   **16**
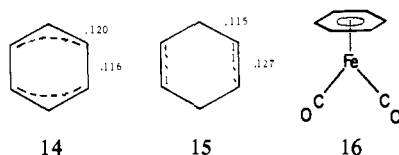
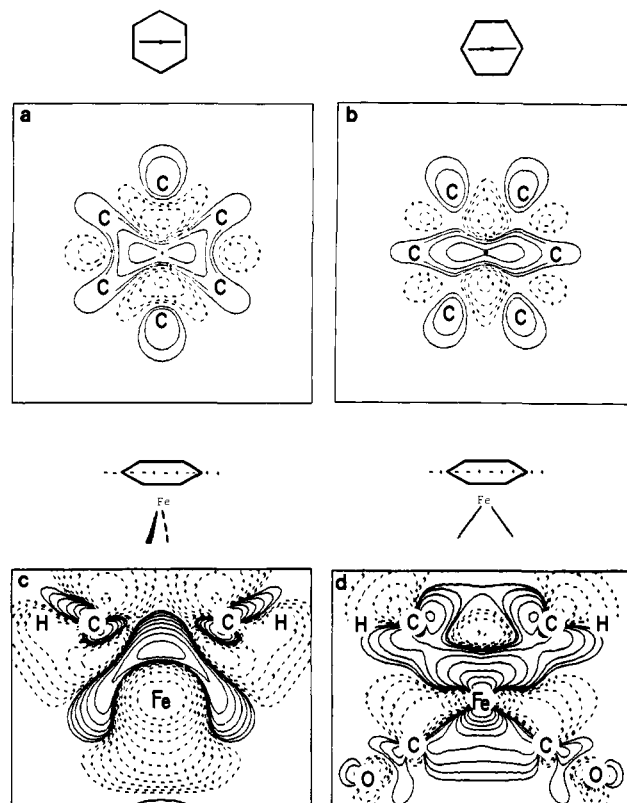(42) Fitzpatrick, N. J.; Mathews, M. J. *J. Organomet. Chem.* **1973**, *61*, C45.

Figure 3. Fragment deformation density plots for $(Bz)Fe(CO)_2$ in the staggered and eclipsed conformations. Maps a and b are for the π-maximum planes. Map a is the staggered conformation, and map b is the eclipsed conformation. Maps c and d are in the vertical C–H plane. Map c is the staggered conformer and contains the atoms in the ring while bisecting the ML_2 group. Map d is the eclipsed conformer and contains both the ring atoms and the ML_2 group.

MO calculations on the staggered and eclipsed conformers of $(\eta^6\text{-}C_6H_6)Fe(CO)_2$, **16**, agreed with these predictions. Both the π-maximum $\Delta\rho$ plots (Figure 3a,b) and the π-overlap populations (shown above) reflect the expected interruption of conjugation in the Bz fragment by the $Fe(CO)_2$ moiety. Hoffmann has suggested[1b] (and we would also expect) that the staggered conformation would be favored by electron-donating (D) groups in ortho and meta positions or electron-withdrawing (A) groups in para positions because the carbonyls would rotate to the most electron-rich sites (viz., **17**). Remember that similar features

17   **18**
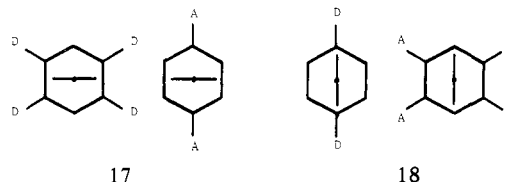
were observed in the crystal structures of substituted (Bz)ML$_3$ complexes[28,38] and reflected in the solution chemistry of such complexes.[39,40] Likewise, the eclipsed conformer would be favored by reversing the order of electron-donating and -accepting groups, as in **18**. Although no such simple complexes like **17** are known, a few studies on BzML$_2$, where L is a perfluorophenyl ligand and the geometry is staggered, do indicate the expected bond length variation.[43]

In these studies, the authors also found that the para positions tended to bend away from the metal to give a puckered structure, **19**. This is not unexpected[43b] and is observed in a $\Delta\rho$ plot of that

19
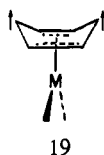
plane for (Bz)Fe(CO)$_2$ (Figure 3c). Here the positive density contours are directed up and away from the Fe(CO)$_2$ group. The atoms in this region should want to deform toward the area of greatest electron density, hence the puckering. We would also expect that the substituents on the eclipsed carbons in conformer **13** (and maybe the carbons themselves) might bend down toward the ML$_2$ fragment, for we see the electron density deforming in this direction in the other plot in Figure 3d.

Two ideal conformations would also be expected for (Bz)ML$_4$ systems such as (Bz)Ti(CO)$_4$ or (Bz)Cr(CO)$_2$(CN)$_2$ (i.e., **20** and **21**). A conformation like **20** would have two long bonds and four shorter bonds, with the long bonds being the ones most eclipsed by the L groups. Such a structure might have an electronic deformation as in **14**. The staggered conformer **21** should have

20   **21**
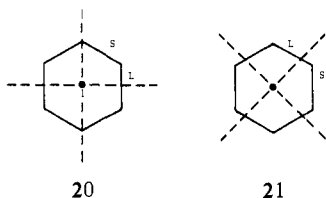
four long bonds and two shorter ones, giving it an electronic arrangement as in **15**. No complexes of this type are known, although we suggest the ML$_4$ (L the same) systems might favor conformation **21**, whereas ML$_2$L'$_2$ (having C_{2v} symmetry) might favor the eclipsed form **20** so that the complex would retain C_{2v} symmetry. However, this is simply speculation and further comment will have to await the preparation and structural characterization of such complexes.

η^5-Cyclopentadienyl (Cpd) Complexes. Probably no other olefin is complexed to as many different metal fragments as is the cyclopentadienyl (Cpd) ligand. It is also probably the least structurally characterized of the cyclic polyenes when bound to ML$_n$ fragments, partly because it is so common a ligand but principally because emphasis is usually placed on refining the other components of a Cpd complex whose structure is being studied. Although all three of the main representatives of the (Cpd)ML$_n$ class have been synthesized—(Cpd)Co(CO)$_2$, **6a**, (Cpd)Mn(CO)$_3$, **5a**, and (Cpd)V(CO)$_4$, **22a**—not all have been fully characterized.[19,21,22,23,44]
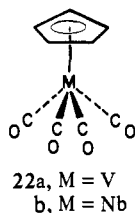
22a, M = V
b, M = Nb

(43) (a) Radonovich, L. J.; Klabunde, K. J.; Behrens, C. B.; McCollor, D. P.; Anderson, B. B. *Inorg. Chem.* **1980**, *19*, 1221. (b) Radonovich, L. J.; Koch, F. J.; Albright, T. A. *Inorg. Chem.* **1980**, *19*, 3373.
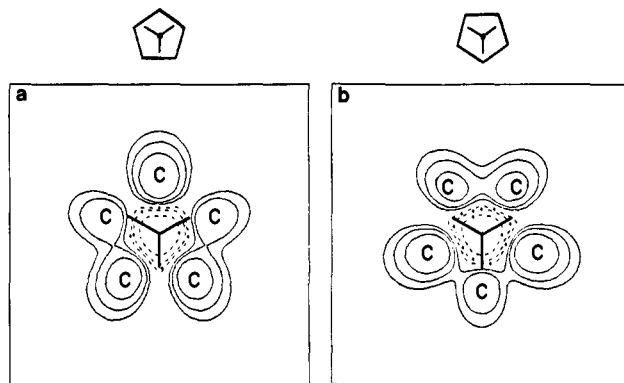
Figure 4. Fragment deformation density plots for (Cpd)Mn(CO)$_3$ in the staggered and eclipsed conformations. The maps depicted are for the π-maximum plane. Map a is the staggered conformation, and map b is the eclipsed conformation.

Part of the reason for the lack of accurate Cpd C–C bond length data is that the five-membered ring has a very low barrier to rotation about the ML$_n$ axis (essentially zero),[1a] which is manifested either in high thermal motion (libration) for the Cpd carbons within the molecule or in disorder of the Cpd ligand throughout the crystal.[44,45] There are several ways to reduce this problem, one of which is to completely methylate the Cpd ligand. This not only aids in crystal growth but also reduces librational and rotational motion substantially.[23b] Similarly, one could increase the rotational barrier by attaching a single substituent to the Cpd ring to force the complex into a particular conformation[46] (as was illustrated with the arene complexes in the previous section). Finally, one could substantially lower the activation energy for rotation by solving the crystal structure at very low temperature.[21b] The first technique (permethylation) resulted in a detailed analysis of **6a**,[23b] while the latter process (low temperature) was used to give the most unambiguous structure of **5a** to date.[21b]

If we consider the (Cpd)ML$_3$ systems, we see that there are two main ideal conformations—the staggered **23** and eclipsed **24**.

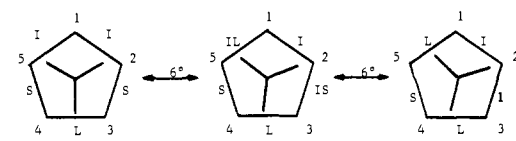**23**   **25**   **24**
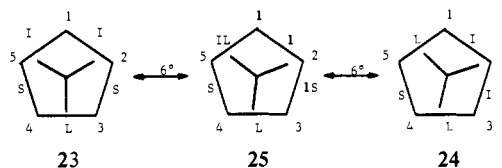
Based upon the principle derived in the last section that C–C bonds eclipsed by carbonyls (or congeners thereof) will be longer than uneclipsed bonds, we would expect that a complex in conformation **23** would display three different sets of bond lengths—one long, two intermediate, and two short (L, I, and S in the drawing)—where the medium length C–C bonds are not eclipsed as much as the longest one. Similarly, a structure like **24** would also be expected to have three sets of bond lengths—one short, two intermediate, and two long—but here the number of long and short bonds is reversed. In each case, the longest bonds would be those most eclipsed by carbonyls (i.e., their conjugation with the other ring carbons is disrupted or interrupted by the greatest amount), and the shortest bonds would be least eclipsed.

Calculations on **5a** in both conformations bear this out. Figure 4 represents fragment deformation density plots of the π-maximum plane in staggered and eclipsed **5a**. The π-overlap populations for the same molecule are given in Table IV. Although the

(44) Wilford, J. B.; Whitla, A.; Powell, H. M. *J. Organomet. Chem.* **1967**, *8*, 495.

(45) See, for example: (a) Carter, O. L.; McPhail, A. T.; Sim, G. A. *J. Chem. Soc. A* **1966**, 1095. (b) Greenhough, T. J.; Kolthammer, B. W. S.; Legzdins, P.; Trotter, J. *Inorg. Chem.* **1979**, *18*, 3548. (c) *Acta Crystallogr., Sect. B* **1980**, *B36*, 795.

(46) See, for example: (a) Harrison, W.; Trotter, J. *J. Chem. Soc., Dalton Trans.* **1972**, 678. (b) Khotsyanova, T. L.; Kuznetsov, S. I.; Bryukhova, E. V.; Makarov, Yu. V. *J. Organomet. Chem.* **1975**, *88*, 351.

Polyenes Bound to Transition-Metal Fragments

J. Am. Chem. Soc., Vol. 105, No. 15, 1983 4937

Table IV. Calculated π-Overlap Populations of the C–C Bonds in (Cpd)Mn(CO)$_3$

conformn	C_1–C_2	C_2–C_3	C_3–C_4	C_4–C_5	C_5–C_1
23	0.117	0.123	0.114	0.123	0.117
24	0.121	0.121	0.115	0.124	0.115
25[a]	0.119	0.122	0.1145	0.1235	0.116

[a] Represents an average of the values obtained for 23 and 24.

π-density differences are not as large as those for (Bz)Cr(CO)$_3$, both the plots and populations point out the expected trend in C–C bond lengths for (Cpd)ML$_3$ complexes. Unfortunately, both 5a and 5b do not crystallize into strictly one conformation or the other. Rather, they display a conformation halfway between staggered and eclipsed, 25.[19,21,22] A population composite of 23 and 24 would suggest that 25 would show five different bond lengths with the relative order shown in Table IV. However, the room-temperature studies of 5a and 5b do not display the calculated trend, nor do they indicate consistent placement of the longest and shortest bonds, even when the statistical error in the bond lengths is small[21a] (see Table V). When the structure of 5a is solved at low temperature (115 K), most of the ambiguity in the bond lengths is removed (Table V, third column). Even though the order of the intermediate length bonds are reversed, there exist the required three sets of bond lengths—one short, two long, and two of medium length. Furthermore, they are located in the expected positions for conformer 24 (as indicated by the averages).

Structures have also been reported for the isoelectronic species (Cpd)Cr(CO)$_2$(NO), 26a,[47] and [(Cpd)Fe(CO)$_3$]$^+$, 26b.[48] Both appear to crystallize in the eclipsed conformation. Although the

26a, M = Cr, L = NO
b, M = Fe$^+$, L = CO
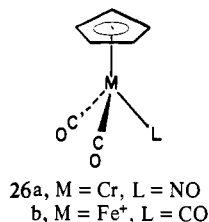
bond length differences border on statistical significance,[10] we will consider their averages (Table V). As stated above, we expect one short, two long, and two intermediate length bonds for 24. Only 26a correctly places the shortest bond trans to the eclipsing ligand. The relative bond order in 26a is also correct, although the disorder in the nitrosyl and carbonyls precludes us from commenting on the relative interrupting ability of CO vs. NO in this case. 26b is another story. The order of medium and long bonds is reversed from what it should be, and one bond is disproportionately longer than the others. Closer examination of this structure reveals that the counterion PF$_6^-$ is exhibiting a significant perturbation on the cationic iron complex. In fact, the anion is located next to and below this bond and is probably either changing the electron density in that bond, making it weaker and, thus, longer or spreading those carbons apart by steric repulsion. To compensate for any density loss, the affected carbons would tend to deform toward the iron to pick up electron density. This is what is observed.

The inconsistency and lack of precision (in many cases) in the data for these Cpd complexes point to a genuine need for further structural studies on these species at low temperature and/or with neutron diffraction, and it may turn out that low temperature will be the most important requirement. Certainly, further studies
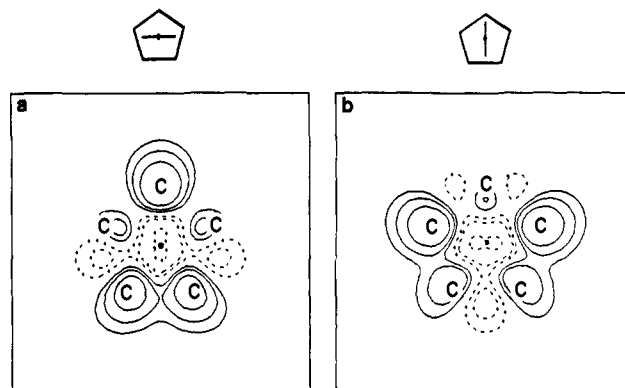

Figure 5. Fragment deformation density plots for (Cpd)Co(CO)$_2$ in both the staggered and eclipsed conformations. The π-maximum plane is depicted.

should be conducted by using the pentamethylcyclopentadienyl ligand, for this would lessen the chances for ring disorder in the crystal as well as reducing the librational motion.

(Cpd)ML$_2$ complexes can also show two conformations 27 and 28. The bond length pattern for 27 will be the same as for structure 24 (one short, two long, two intermediate), whereas 28

27   28
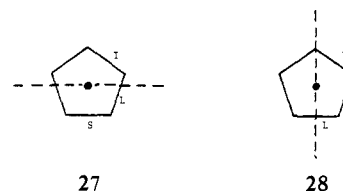
will display the pattern for structure 23 (one long, two short, two intermediate). Pictorially, we can represent the electron density localizing for 27 according to the pattern in 29. Similarly, an electron density localization for 28 might look like 30. A cal-

29   30
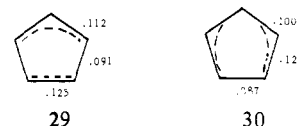
culation on (Cpd)Co(CO)$_2$, 6a, produced π-overlap populations (shown on 29 and 30) and $\Delta\rho$ plots (Figure 5) consistent with these expectations. In fact, this is just what is observed experimentally for the staggered structure in the pentamethyl analogue of 6a, where the short, long, and intermediate pattern is found with values of 1.392, 1.446, and 1.410 Å ($\sigma = \pm 0.006$ Å) for the C–C bond lengths.[23b] A similar pattern is also observed in (C$_5$H$_4$NO$_2$)-Rh(CO)$_2$ (which also has the staggered form), although the bond lengths were not as precisely determined.[50]

Although a (Cpd)ML$_2$ complex in the eclipsed conformation has not been determined, Beagley et al. found that a model of 6a with one of the carbonyls nearly eclipsing one of the ring carbons gave a better fit to their electron diffraction data than did a staggered model.[23a] An eclipsed structure in the solid state might be obtained in one of two ways. One could make one of the counterligands different, as in (Cpd)Fe(CO)(NO), or put a single electron-donating substituent on the ring, as in (C$_5$H$_4$Me)Co(CO)$_2$ [Me = methyl]. Both complexes might tend to rotate into eclipsing conformations, either to maintain C_{2v} symmetry in the molecule (i.e., for the iron complex) or to eclipse the electron density enhanced carbon in the cobalt complex. As was found in (C$_5$-H$_4$NO$_2$)Rh(CO)$_2$, substituting an electron-withdrawing substituent on the ring forces the complex into the staggered form.

Albright and Hoffmann have discussed the conformational preferences of (Cpd)ML$_n$ complexes in detail,[51] and our findings

(47) Atwood, J. L.; Shakir, R.; Malito, J. T.; Herberhold, M.; Kremnitz, W.; Bernhagen, W. P. E.; Alt, H. G. *J. Organomet. Chem.* 1978, 165, 65.

(48) Gress, M. E.; Jacobson, R. A. *Inorg. Chem.* 1973, 12, 1746.

(49) Hubbard, J. L.; Lichtenberger, D. L. *Inorg. Chem.* 1980, 19, 1388.

(50) Rausch, M. D.; Hart, W. P.; Atwood, J. L.; Zaworotko, M. J. *J. Organomet. Chem.* 1980, 197, 225.

(51) Albright, T. A.; Hoffmann, R. *Chem. Ber.* 1978, 111, 1578.

4938   *J. Am. Chem. Soc., Vol. 105, No. 15, 1983*

Chinn and Hall

Table V.   C–C Bond Length Summary for Some $(Cpd)M(CO)_2(XY)$ Complexes[a]

	M = Mn XY = CO	M = Mn[b] XY = CO	M = Mn[c] XY = CO	M = Re[b] XY = CO	M = Cr XY = NO	M = Fe^{+} XY = CO
C_1–C_2	1.433 (1.418)[d]	1.416 (1.428)	1.403 (1.406)	1.387 (1.415)	1.392 (1.383)	1.428 (1.396)
C_2–C_3	1.404	1.439	1.408	1.443	1.374	1.363
C_3–C_4	1.399 (1.392)	1.434 (1.428)	1.418 (1.418)	1.438 (1.430)	1.398 (1.392)	1.338 (1.352)
C_5–C_1	1.385	1.421	1.417	1.421	1.387	1.366
C_4–C_5	1.350	1.400	1.399	1.400	1.365	1.355
σ	0.02	0.003	0.003	0.02	0.008	0.013
conformer	25	25	25	25	24	24
ref	19	21a	21b	22	47	48

[a] Bond lengths are in Å. Data for structures collected at room temperature unless otherwise noted. [b] Values corrected for libration. [c] Data collected at 115 K. [d] Values in parentheses are simple averages of the two bond lengths immediately above and below the average value.

agree with their predictions. However, they predict that $(Cpd)ML_2$ complexes in the staggered conformation **31** should slip slightly from η^5 to more η^2 bonding (the η^2 slip) **32**. Thus,
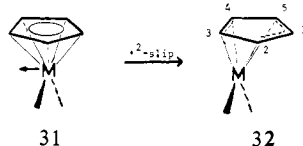
the metal should be nearer the 3,4-positions than the 1,2,5-carbons. In the structure of **6b** by Byers and Dahl,[23b] it was reported that carbons 1,3,4 were equidistant to the cobalt [average 2.103 (4) Å] and that carbons 2 and 5 were also equidistant [2.067 (5) Å] but closer. So, rather than undergoing an η^2 slip, the $Co(CO)_2$ group has drawn the 2,5-positions closer to itself.

For $(Cpd)ML_4$ complexes in the staggered and eclipsed conformations, one would predict the bond orders as shown in **33** and **34**. Both $(Cpd)V(CO)_4$, **22a**, and the isolobal niobium complex
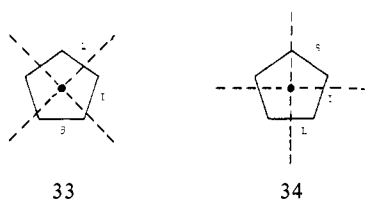
22b have been partly characterized and both crystallize in the staggered conformer. However, **22a** is disordered (although one of the Cpd rings does show the expected pattern),[44] and the bond length results for **22b** were never published.[52] Both would be good candidates for further study at low temperature and/or with the C_5Me_5 ligand. Although not yet known, good candidates for structures in the eclipsed form might be $(Cpd)Ti(CO)_3(NO)$, $(C_5H_4Me)V(CO)_4$, or $(Cpd)Cr(CO)_3(CN)$.

η^4-**Cyclobutadiene (Cbd) Complexes.** Though the chemistry of complexed cyclobutadiene is extensive,[53] structural studies are few[20,29,54] and raise some interesting questions which need to be answered. The main representative of the $(Cbd)ML_3$ complexes $(\eta^4$-$C_4H_4)Fe(CO)_3$, **7a**, has been studied by electron diffraction[20b] but not by X-ray diffraction. Unfortunately, the gas-phase study did not reveal any preferred conformation of the Cbd ring, bond length variations, or any displacement of the hydrogens from the Cbd plane. An early X-ray study of the tetraphenyl derivative **7b**[20a] revealed the structure summarized in Table VI.

(52) Doedens, R. J.; Dahl, L. R. *J. Am. Chem. Soc.* **1965**, *87*, 2576.
(53) See, for example: (a) Maitlis, P. M. *Adv. Organomet. Chem.* **1966**, *4*, 95. (b) Maitlis, P. M.; Eberius, K. W. In "Non-Benzenoid Aromatics"; Snyder, J. P., Ed.; Academic Press: New York, 1971; Chapter 6. (c) Pettit, R. *J. Organomet. Chem.* **1975**, *100*, 205. (d) Efraty, A. *Chem. Rev.* **1977**, *77*, 691 and references therein.
(54) (a) Cash, G. G.; Helling, J. F.; Mathew, M.; Palenik, G. J. *J. Organomet. Chem.* **1973**, *50*, 277. (b) Riley, P. E.; Davis, R. E. *Ibid.* **1977**, *137*, 91. (c) Davis, R. E.; Riley, P. E. *Inorg. Chem.* **1980**, *19*, 674 and references therein.

Table VI. Crystal Structure Summary of $(C_4Ph_4)Fe(CO)_3$[20a]

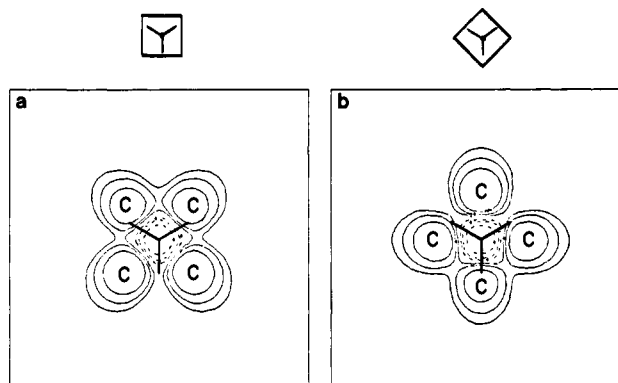| conformatn	bond lengths, Å actual	av	Ph bend, deg actual	av
	C_1–C_4 = 1.469 (17) C_1–C_2 = 1.468 (17)	1.468	Ph_1 = 16.7 Ph_2 = 6.9	
	C_3–C_2 = 1.454 (17) C_3–C_4 = 1.445 (17)	1.450	Ph_4 = 10.1 Ph_3 = 9.6	8.5
	Fe–C_1 = 2.055 (12) Fe–C_2 = 2.054 (12) Fe–C_4 = 2.069 (13) Fe–C_3 = 2.091 (12)	2.062		

Figure 6. Fragment deformation density plots for $(Cbd)Fe(CO)_3$ in the staggered and eclipsed conformations. The maps shown are for the π-maximum plane. Map a is the staggered conformation, and map b is the eclipsed conformation.

As can be seen, the data indicate that the complexed Cbd has three types of bonds—two long, one intermediate, and one short—and displays the eclipsed conformation **35**. Yet, all the
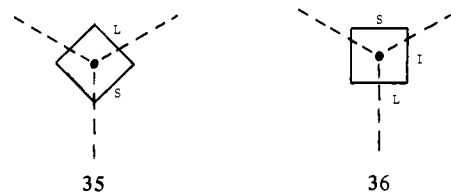
C–C bond lengths are within two esd's of one another and should properly be classified as equal, which the authors do. But are they equal, and if not, what is the correct ratio? The results of the $(Bz)ML_n$ and $(Cpd)ML_n$ studies would indicate that conformation **35** should give only two sets of bonds, two long and two short, with the long ones eclipsed by the carbonyls. Similarly, the staggered conformation **36** would have three types of bond lengths, but the ratio would be different: one long, two intermediate length, and one short.

To provide a basis for deciding the issue, calculations were performed on **7a** in both conformations and fragment deformation densities computed. The $\Delta\rho$ maps for the π-maximum planes are

shown in Figure 6. The plots confirm the expected bond order outlined above. We can conclude from this that **7b** really should have only two types of bonds, two equal long ones and two equal shorter ones, with the long bonds being eclipsed by the carbonyls. Thus, the two long bonds in the structure really are equal (average 1.468 Å) and should be different from the other two C–C bond lengths, which should be shorter (average 1.450 Å) and are also equal. It is interesting that the data gave better results than the statistics should have allowed. Redone at low temperature with modern X-ray instrumentation, this complex and its parent **7a** should both show C_s symmetry and have two sets of C–C bond lengths.

These geometrical distortions are important for several reasons. First, one needs to be aware of their possible existence when solving diffraction or vibrational data: i.e., making an assumption that the complexed Cbd is square may or may not be valid, depending on the particular experiment being conducted. Second, cognizance by theoretical chemists of possible nonsquare-complexed Cbd would be very important in any geometry study. This was, at least, deemed worth considering in a recent work by Herndon.[55a] However, Anderson and Fitzgerald conclude in a comparison of square with rectangular Cbd that Cbd must be square on complexation to $Fe(CO)_3$.[55b] They ignored the possibilities, suggested here, that it might be trapezoidal (staggered conformation) or diamond-shaped (eclipsed conformation).

For $(Cbd)ML_2$ complexes such as $(Cbd)Fe(NO)_2$, **37a**, or $(Cbd)Ni(CO)_2$, **37b**, we expect to have two main conformations **38** and **39**. As with the $(Bz)ML_3$ complexes, we again have one

37a, M = Fe, L = NO
  b, M = Ni, L = CO

38   39
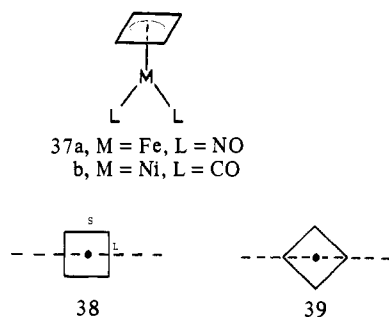
fragment of low symmetry (C_{2v}) being imposed over another of higher symmetry (D_{4h}). Thus, the distortions in the bonds for the staggered conformation should be large. Both complexes show a definite density loss from the eclipsed C–C bonds, implying that this conformer should represent a *rectangular* Cbd!

This would suggest an electronic structure for this conformer like **40** with two localized olefinic bonds.[1b] By analogy to eclipsed $(Bz)ML_3$, we expect to find no bond length differences in the eclipsed conformation of **37**, and this is what the calculation shows. However, clearly there is electron density rearrangement to give an electronic structure like **41**, which would, presumably, yield a diamond-shaped Cbd, which could then pucker into a butterfly shape.


40   41

Hoberg and co-workers[56] have made a number of tetramethyl and tetraphenyl $CbdNiL_2$ complexes but not with simple π acceptor ligands like CO. Both Hoffmann and co-workers[1b] and Bursten and Fenske[57] have indicated the stability of $(Cbd)Ni(CO)_2$ to be low.

In terms of orientation, the ML_2 group should rotate away from electron-withdrawing (A) substituted positions and toward elec-

tron-donating (D) positions, **42**, as was found for the $(Bz)ML_3$ systems. Then, in the eclipsed conformer, nucleophiles would attack the uneclipsed (electron density rich) carbons, while electrophiles would preferentially attack the eclipsed (electron density poor or depleted) carbon sites.


42
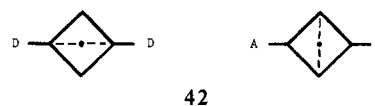
For $(Cbd)ML_4$ complexes such as $(Cbd)M(CO)_4$ [M = Cr, Mo, W], **43**, all of which have been prepared,[58] but none of which have been structurally characterized, there are the usual two conformations **44** and **45**. Neither will show any bond length

43   44   45
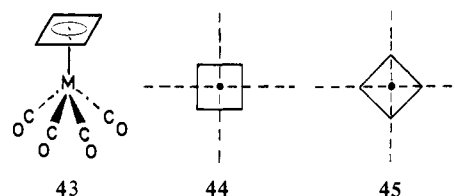
alternation, and both will show a square Cbd ligand if the ML_4 group has C_{4v} symmetry. In those instances in which the ML_4 fragment distorts to C_{2v} symmetry, **46**, or for symmetrical $ML_2L'_2$ fragments [i.e., $Fe(CO)_2(CN)_2$ or $Ti(CO)_2(NO)_2$], the complexed Cbd might be expected to show bond alternation in conformer **44** but not in **45**.

46
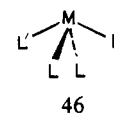
η^3-Cyclopropenyl (Cpp) Complexes. Only a handful of η^3-Cpp complexes have been prepared and structurally characterized.[59] Of interest to this study is the parent complex for the $(Cpp)ML_3$ compounds $(\eta^3-C_3H_3)Co(CO)_3$, **47a**. Again, such a complex could be in one of two conformations **48** and **49**; and, like the $(Cbd)ML_4$

47a, R = H   48   49
  b, R = C_6H_5
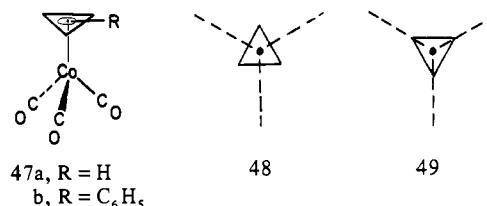
conformers, there will be no bond length differences in either conformation. This is borne out in the structure of **47b** (the triphenyl derivative of **47a**), which has equal C–C bond lengths within two esd's and the staggered conformation. The distortions from ideal symmetry are probably due to the steric crowding of the phenyl groups within the crystal. Indeed, the longest Cpp C–C bond is between two carbons which have been pushed closer to the eclipsing carbonyl counterligand and agrees with the expected behavior of eclipsing bonds being longer, the greater the interaction.

Of greater interest are the $(Cpp)ML_2$ complexes, represented in this study by $(Cpp)Co(NO)_2$, **50**. Both conformations **51** and **52** would have C–C bond deformations: two long and one short in **51**, producing an electronic structure like **53** (a coordinated cyclopropene); one long and two short in **52**, yielding an electronic arrangement like **54** (allylic-like). The $\Delta\rho$ plots for the π-max-

(55) (a) Herndon, W. C. *J. Organomet. Chem.* **1983**, *232*, 1633. (b) Anderson, A. B.; Fitzgerald, G. *Inorg. Chem.* **1981**, *20*, 3288.

(56) Hoberg, H.; Richter, W.; Fröhlich, C. *J. Organomet. Chem.* **1981**, *213*, C49 and references therein.

(57) Bursten, B. E.; Fenske, R. F. *Inorg. Chem.* **1979**, *18*, 1760.

(58) Amiet, G.; Reeves, R. C.; Pettit, R. *J. Chem. Soc., Chem. Commun.* **1967**, 1208.

(59) (a) Tuggle, R. M.; Weaver, D. L. *Inorg. Chem.* **1971**, *10*, 1504. (b) *Ibid.* **1971**, *10*, 2599. (c) McClure, M. D.; Weaver, D. L. *J. Organomet. Chem.* **1973**, *54*, C59. (d) Chiang, T.; Kerber, R. C.; Kimball, S. D.; Lauher, J. W. *Inorg. Chem.* **1979**, *18*, 1687. (e) Mealli, C.; Midollini, S.; Moneti, S.; Sacconi, L.; Silvestre, J.; Albright, T. *J. Am. Chem. Soc.* **1982**, *104*, 95.

50   51   52
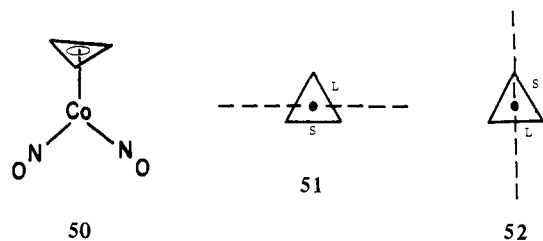
imum planes (Figure 7) concur with this expectation.

53   54

Hoffmann and co-workers also suggest the tendency for the (Cpp)ML$_2$ complexes to undergo the η^2 slip from η^3 bonding.[1b,60] Though the π-maximum maps do not suggest a direction, we might expect that the ML$_2$ fragment would slip toward the carbons with the stronger bonds and greatest density, i.e., toward the uneclipsed bond, 55, and toward the eclipsed carbon, 56. In the first instance,

55   56
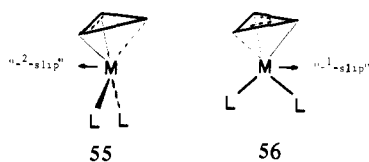
motion toward η^2 bonding with the olefinic bond would weaken it (relative to the other two) and lengthen it. The resulting electronic structure would be as in 54. This is exactly what is found in the structure of [(C$_3$Ph$_3$)Pt(PH$_3$)$_2$]$^+$, Ph = phenyl, which has the staggered conformation 57.[59c] In the second instance,

57
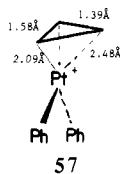
motion toward η^1 bonding with the eclipsed carbon would reduce the interaction with the trans bond, making it stronger and shorter. Then, 53 becomes more important as the complex approaches being a σ-bonded cyclopropene.

(Cpp)ML$_4$ complexes such as (Cpp)Mn(CO)$_4$ might have two short bonds in the staggered conformation 58 and two long bonds in the eclipsed conformation 59. The resulting electronic ar-

58   59
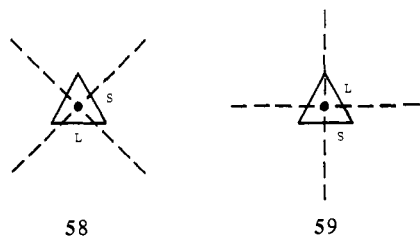
rangements would be allylic-like (54) for 58 and cyclopropene-like (53) for 59. No such compounds have been prepared, but (η^3-C$_3$Ph$_3$)V(CO)$_5$[61] might prove to be a good candidate for study if the V(CO)$_5$ group has local C_{4v} symmetry.

η^7-Cycloheptatrienyl (Cht) Complexes. There is a genuine paucity of Cht complexes prepared and structurally characterized,[62] and only two can be considered in light of this work: (η^7-C$_7$H$_7$)V(CO)$_3$, 60a,[63] and [(η^7-C$_7$H$_7$)Mo(CO)$_3$]$^+$, 60b.[62a]

(60) Jemmis, E. D.; Hoffmann, R. *J. Am. Chem. Soc.* 1980, *102*, 2570.
(61) Schneider, M.; Weiss, E. *J. Organomet. Chem.* 1976, *121*, 345.
(62) (a) Clark, G. R.; Palenik, G. J. *J. Organomet. Chem.* 1973, *50*, 185. (b) Zeinstra, J. D.; DeBoer, J. L. *Ibid.* 1973, *54*, 207. (c) Mohr, D.; Wienand, H.; Ziegler, M. L. *Ibid.* 1977, *134*, 281 and references therein.
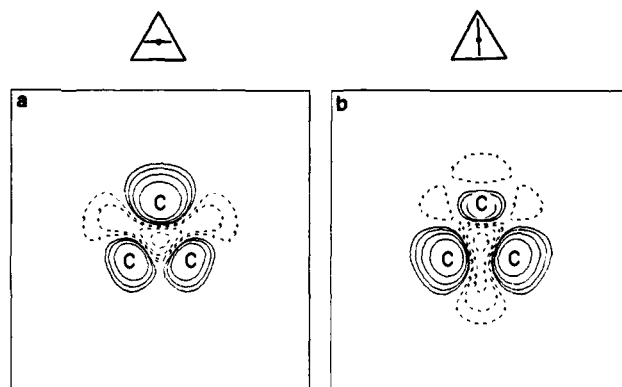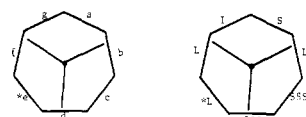

Figure 7. Fragment deformation density maps for the staggered and eclipsed conformations of (Cpp)Co(NO)$_2$ in the π-maximum plane. Map a is the staggered, and map b is the eclipsed form.

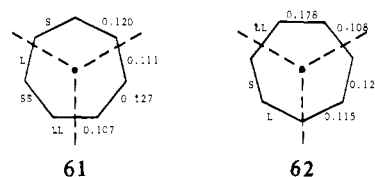Table VII. Bond Length (Å) Data for [(Cht)Mo(CO)$_3$]BF$_4$[62a]

$a = 1.378$ (18)	$e = 1.409$ (18)
$b = 1.415$ (14)	$f = 1.408$ (18)
$c = 1.368$ (17)	$g = 1.396$ (17)
$d = 1.425$ (17)	

Unfortunately, the full structure of 60a has never been published, merely an indication of the planarity of the ring and the metal-to-ring distance.[63] The two possible ideal conformations for these

60a, M = V
  b, M = Mo$^+$

61   62
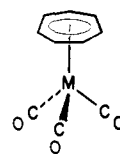
(Cht)ML$_3$ complexes would be 61 and 62. Both conformers would have four possible sets of bond lengths, with the relative orders indicated (SS = shortest, S = short, L = long, LL = longest). The calculated π-overlap populations for 60a in both conformers are also included in the drawings. They agree quite well with the observed π-maximum $\Delta\rho$ plots (not shown).

The C–C bond lengths for 60b are given in Table VII. As was the case for the (Cpd)ML$_3$ complexes, the Mo(CO)$_3$ group seems to be situated halfway between staggered and eclipsed (a value for the rotation angle was not given). If we average the overlap populations for 61 and 62, we get an intermediate set of overlap populations for the conformer halfway between 61 and 62 (viz., 63). With the exception of the starred (*) bond (also see Table VII), the bond lengths fit perfectly with this composite bond order. The one exception *should* be one of the shortest bonds and not a long bond. However, upon closer examination of the structure, we find that the counterion in this structure, BF$_4^-$, is situated below this C–C bond and is almost certainly causing the anomalous

(63) Allegra, G.; Perego, G. *Ric. Sci., Parte 2: Sez. A* 1961, *1*, 362.

$1a_{2u}$ $1e_{1g_1}$ $1e_{1g_2}$

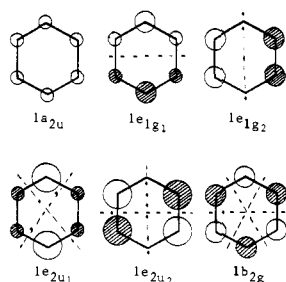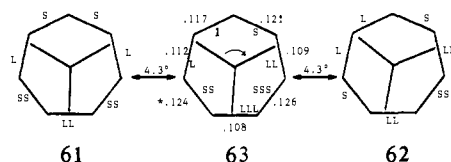$1e_{2u_1}$ $1e_{2u_2}$ $1b_{2g}$

Figure 8. Pictorial representation of the π orbitals of benzene.

behavior in this bond length, by either steric repulsion or electronic interaction.

61   63   62

Theoretical Analysis

We have seen that deformation densities obtained by subtracting the total density of the fragments from that of the complex yield pictorial descriptions of incipient nuclear motion. In particular, $\Delta\rho$ plots in the π-maximum planes of $(C_nH_n)ML_m$ complexes indicate potential C–C bond length changes, and these electron density deformations often correlate well with the simple overlap populations within the polyene p_π framework. But, what are the detailed orbital interactions which are causing these shifts in electron density?

The density matrix for a system of n doubly occupied molecular orbitals is

$$D_{ab} = 2\sum_i^n C_{ia}C_{ib} \qquad (2)$$

where C_{ia} is the coefficient of the atomic orbital a in the molecular orbital i. The overlap population between two atomic orbitals, a and b, is simply the density matrix element D_{ab} times the overlap integral S_{ab}. Thus, any change in the overlap population of the π system of a regular polyene will be reflected in changes of the density matrix elements. In many cases it is easier to view the change in these densities by examining the density matrix in the molecular orbital basis of the individual fragments. The transformation between the density matrix in the atomic orbital basis, D_{ab}, and that in the fragment orbital basis, $W_{\sigma\rho}$ is given in eq 3, where $V_{\sigma a}$ is the coefficient of atomic orbital a in fragment orbital σ.

$$D_{ab} = \sum_\sigma\sum_\rho W_{\sigma\rho}V_{\sigma a}V_{\rho b} \qquad (3)$$

The fragment orbitals for the π system of benzene are shown pictorially in Figure 8 where the sizes of the circles represent the relative size of the coefficient of the p_π atomic orbital. In free benzene the $W_{\sigma\rho}$ coefficients are 2.00 for the diagonal terms of the three occupied molecular orbitals, $1a_{2u}$, $1e_{1g_1}$, and $1e_{1g_2}$ and zero otherwise. When the benzene molecule bonds to a transition-metal fragment, these $W_{\sigma\rho}$ terms will change reflecting the new electron distribution. In $(Bz)Cr(CO)_3$ the $1e_{1g}$'s lose electron density (donation to the metal) while the $1e_{2u}$'s gain electron density (accepting from the metal). Because the tricarbonyl fragment preserves the threefold symmetry, the two e_{1g} and e_{2u} orbitals are both e and can mix. It is this mixing that gives rise to off-diagonal W terms and to the bond alternation. It is the interaction of the Bz e_π orbitals with, principally, the ML_3 10e orbitals (mostly $d_{x^2-y^2}$ and d_{xy} in character) which mixes the bonding, e_{1g}, and antibonding, e_{2u}, Bz MO's to give the observed C–C bond length alternation.

In a molecule like $(Cpd)Co(CO)_2$ the symmetry is reduced to the point that the two e components are no longer degenerate and can have different diagonal $W_{\sigma\sigma}$ terms. In this case the perturbation may be viewed as a higher order effect, and the observed distortion is larger.

Conclusions

Several important conclusions can be derived from these results. We have seen that ML_n (L being a σ-donating/π-accepting ligand) fragments in general and $M(CO)_n$ fragments in particular tend to interrupt the π-bond delocalization in complexed cyclic polyenes. The interruption causes electron density to flow from the eclipsed C–C bonds to those not eclipsed or eclipsed to a lesser extent, and the resultant density loss (gain) causes bond lengthening (shortening).

We have found that the bond alternation has its roots in the first-order coupling of the ML_3 10e or the ML_2 $12a_1$ and $2a_2$ fragment MO's with the polyene e_π orbitals. This interaction mixes various amounts of the bonding, nonbonding, and antibonding e_π orbitals to produce the observed bond strengthening or weakening.

Finally, we have seen that there exists enough experimental data to confirm our theoretical premise of π-conjugation interruption but not enough to observe its wide applicability. Obviously, there is a genuine need for further X-ray structural determinations on these complexes, and these need to be done at low temperature to reduce thermal libration effects.